

## INFRARED EMISSION FROM M31<sup>1</sup>

H. J. HABING, G. MILEY, E. YOUNG, B. BAUD, N. BOGGESS, P. E. CLEGG, T. DE JONG,  
 S. HARRIS, E. RAIMOND, M. ROWAN-ROBINSON, AND B. T. SOIFER

Received 1983 October 18; accepted 1983 November 18

### ABSTRACT

Maps of M31 have been obtained at wavelengths of 12, 25, 60, and 100  $\mu\text{m}$ . Emission is detected from the center and from a ring of 50' radius. The ring is that also seen in H I, in H II, and in radio continuum radiation. The spectrum of the central emission suggests a hotter dust temperature than in the ring. M31 is a weak infrared source, the radiation measured longward of 12  $\mu\text{m}$  being only 3% of its total luminosity. The two closest companion galaxies, M32 and NGC 205, have also been detected.

*Subject headings:* galaxies: Local Group — infrared: sources

### I. INTRODUCTION

The Andromeda galaxy (M31, NGC 224) is a prime object for observation by *IRAS* because it is nearby (690 kpc) and can be studied in great detail in spite of its large inclination (approximately  $78^\circ$ ). We refer to Sandage and Tammann (1981, hereafter ST) for basic characteristics of the galaxy.

M31 is difficult to observe at IR wavelengths because of its low surface brightness and large angular size. Rieke and Lebofsky (1979) summarize several observations of the central area at  $\lambda \sim 20 \mu\text{m}$ . Telesco and Harper (1980) give an upper limit of 45 Jy at 90  $\mu\text{m}$  for emission from a central area of 50'' diameter.

In this *Letter*, we present preliminary maps of the Andromeda galaxy in all four *IRAS* wavelength bands; a detailed study is under way and will be reported later.

### II. OBSERVATIONS AND REDUCTIONS

We made two adjacent raster scans, each repeated four times and each covering an area of  $3^\circ \times 3^\circ$ . The direction of the scans was almost parallel to the minor axis. Since, in the cross scan direction, the full-sized detectors all have roughly the same size (see Neugebauer *et al.* 1984), the angular resolution parallel to the major axis is the same in all four wavelength bands. In the in-scan direction, i.e., parallel to the minor axis, the resolution is progressively poorer at longer wavelengths (see Fig. 1).

The first maps constructed from individual raster scans were marred by two defects. (1) Baseline variations from detector to detector produced significant intensity stripes parallel to the scan path; the effect was particularly severe in the two short-wavelength maps. (2) All baselines were tilted because of the zodiacal light. Corrections were applied by specially developed "destriping" and "flat-fielding" algorithms.

<sup>1</sup>The *Infrared Astronomical Satellite (IRAS)* used in these observations was developed and is operated by the Netherlands Agency for Aerospace Programs (NIVR), the US National Aeronautics and Space Administration (NASA), and the UK Science and Engineering Research Council (SERC).

### III. RESULTS

In Figure 2 (Plate L6) we show the 60  $\mu\text{m}$  map together with maps taken at very different wavelengths. A similar structure is seen in all four IR maps in Figure 1; it consists of two elements: (1) an extended source at the center and (2) a ring of "spiral arm-like" features with a semimajor axis of approximately 45'. Some weaker spiral arm features are found inside and outside of the ring.

The total flux densities found by integrating the emission over the region of the galaxy as defined by the 100  $\mu\text{m}$  map are given in Table 1; the uncertainties quoted are formal values, based on noise and calibration uncertainties. However, the sloping zodiacal background may have led us to miss some low brightness emission.

Table 1 also contains the integrated flux density of the central regions; its contribution to the total flux is less than a few percent.

### IV. COMPARISON OF IR MAPS WITH PHOTOGRAPHS AND RADIO MAPS

A detailed comparison between the 60  $\mu\text{m}$  map and a IIIa-J plate (taken by A. G. de Bruyn at the 48 inch [1.2 m] Schmidt telescope at Palomar) shows that the spiral arm-like features coincide very closely with prominent dust lanes except for one, which is further discussed below. We conclude that IR radiation by warm dust is the most likely emission mechanism. The IR emission also correlates quite well with the distribution of the H II regions as given by Pellet *et al.* (1978): maxima in the 60  $\mu\text{m}$  map coincide, almost without exception with areas of large and bright H II regions.

Two maps of M31 in the 21 cm line were inspected (Unwin 1980*a, b*; Brinks and Shane 1983; the latter is shown in Fig. 2). Within the ring, the similarity is close: the contours of Unwin's most intense line brightness, corresponding to 1400  $\text{K km s}^{-1}$ , coincide well with the 12  $\mu\text{m}$  IR map (both maps have practically the same angular resolution). The most striking difference is in the absence of atomic hydrogen at the center.

Inward of the ring, two spiral arm-like features clearly seen in the IR show up only faintly in the H I maps. Possibly the

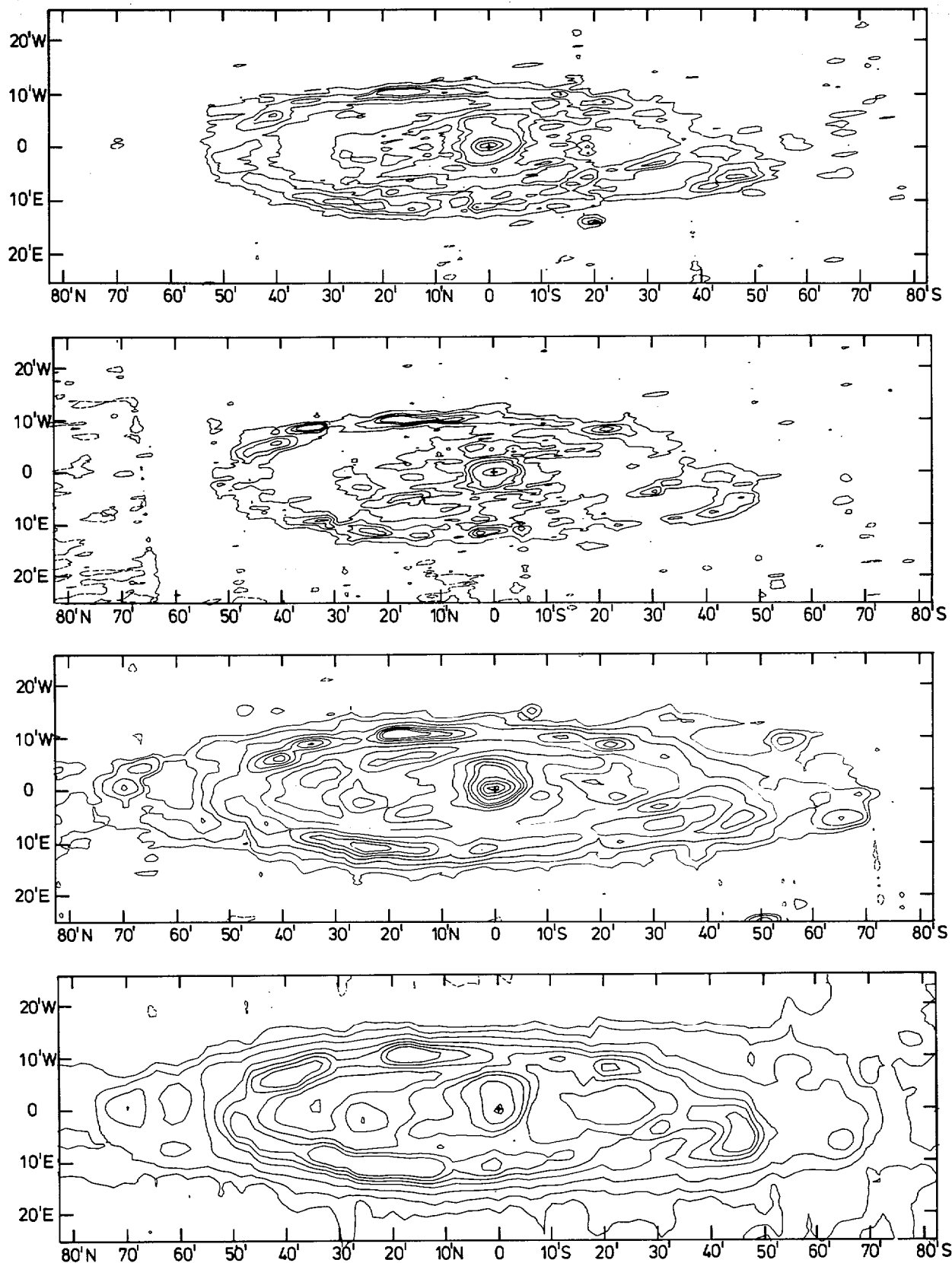


FIG. 1.—The distribution of surface brightness of M31 at the four *IRAS* wavelengths (from top to bottom: 12  $\mu\text{m}$ , 25  $\mu\text{m}$ , 60  $\mu\text{m}$ , 100  $\mu\text{m}$ ). The contour values are expressed in noise units; at 12 and 25  $\mu\text{m}$ , the contour levels are at  $-10, -5, 5, 10, 15, 20, 40, 60, 80, 100, 120$ ; at 60 and 100  $\mu\text{m}$ , contour levels are at  $-10, -5, 5, 10, 20, 40, 60, 80, 100, 150, 200, 250, 300$ . The noise values are, respectively,  $10.8, 4.2, 1.4,$  and  $1.8 \times 10^{-9} \text{ W m}^{-2} \text{ sr}^{-1}$ .

TABLE 1  
SURFACE BRIGHTNESS INTEGRATED OVER SEVERAL AREAS

AREA	FLUX DENSITY (Jy)			
	12 $\mu\text{m}$	25 $\mu\text{m}$	50 $\mu\text{m}$	100 $\mu\text{m}$
Total area .....	170 $\pm$ 60	220 $\pm$ 110	690 $\pm$ 140	3800 $\pm$ 800
Central 3' $\times$ 4.5' ...	4.6	4.1	27.2	55.5
NGC 205.....	< 0.10	< 0.25	0.42	2.12
M32.....	0.40	0.07	...	...

gas is predominantly molecular. L. Blitz (private communication) has measured strong CO emission at one position on one of these arms. Only one of the two features (NW of the nucleus) shows up as a dust lane; the other (SE of the nucleus) is probably behind the bulge of M31.

Maps of radio continuum radiation (Fig. 2; R. Walterbos and P. Schwing, private communication) show a general similarity to the *IRAS* maps. This outcome is not surprising in view of Unwin's (1980*a, b*) conclusion that there is a close correlation between the distributions of H I and H II regions. The radio emission is largely nonthermal except, possibly, at the shortest wavelengths ( $\ll 10$  cm) (Beck and Graeve 1982).

V. DISCUSSION

a) Total Flux

From Table 1 the luminosity between 12 and 100  $\mu\text{m}$  is  $1.5 \times 10^9 L_{\odot}$ . It is likely that this is only a lower limit. First, a significant amount of radiation is probably emitted beyond 100  $\mu\text{m}$  (see Fig. 2). Second, large-scale background emission may have been missed because of the baseline problems. The luminosity of  $1.5 \times 10^9 L_{\odot}$  corresponds to 3% of the luminosity in the visual and in the ultraviolet (ST), but the true value could be a factor of 2-4 larger. In comparison with other spiral galaxies (de Jong *et al.* 1984), M31 is a very weak emitter of IR radiation.

b) Ring Structure

The close agreement between the IR brightness distribution and that of the H II regions excludes the possibility that evolved stars or their circumstellar shells contribute significantly to the measured IR flux. Instead, the agreement indicates that OB associations produce the emission even at the shortest wavelengths. At 12 and 25  $\mu\text{m}$ , our resolution at the distance of M31 corresponds to 900 pc in the direction of the major axis and 150 pc in the direction of the minor axis. Since we do not know the IR emission from comparable areas of similar size in our Galaxy, a direct comparison has not been made.

The overall agreement between the distribution of the radio continuum emission and the IR emission has a rather indirect explanation. Both emissions are caused by the enhanced density of interstellar matter in the ring area. The IR emission is due to enhanced dust densities in conjunction with an increased rate of star formation. The (nonthermal) radio continuum is due to enhanced magnetic fields and, possibly, local sources of relativistic particles (e.g., Berkhuisen, Wielebinski, and Beck 1983).

c) Central Area

Extrapolations from 2.2  $\mu\text{m}$  (Sandage, Becklin, and Neugebauer 1969) and 1.6  $\mu\text{m}$  (Aaronson, Huchra, and Mould 1979) predict about 6 Jy at 12  $\mu\text{m}$  in a 3' diameter beam at the center. Thus the emission at 12  $\mu\text{m}$  is largely due to emission from stellar photospheres. The emission at longer wavelengths is far in excess and must come from warm interstellar grains. For grains with a  $\nu^1$  emissivity, the 60/100  $\mu\text{m}$  flux ratio implies a physical grain temperature of 34 K. This high value can be explained by the strong radiation field at visual wavelengths ( $\lambda > 300$  nm) produced by the high density of late-type giants; the ultraviolet radiation field is definitely too weak (see Coleman, Wu, and Weedman 1980).

For an estimate of the mass of the dust, we adopt an absorption coefficient at 60  $\mu\text{m}$  of  $130 \text{ cm}^2 \text{ g}^{-1}$  (see, e.g., Hildebrand 1983); with a dust temperature of 34 K and a flux density of 27 Jy, we derive a dust mass of  $3000 M_{\odot}$ . If the gas to dust ratio is 100, we obtain a total amount of gas below the detection threshold set by H I and CO measurements (see, e.g., Deharveng *et al.* 1982).

The presence of dust in M31 has been known for several decades from optical photographs (Baade 1963; Hodge 1980). The only direct quantitative estimate, by Gallagher and Hunter (1981),  $M_D \leq 10^6 M_{\odot}$ , agrees with our value. The coincidence with the nonthermal radio radiation from the center is remarkable, but probably fortuitous.

d) Two Companions: NGC 205 and M32

The two companions of M31, NGC 205 and M32, have both been detected. The 12 and 25  $\mu\text{m}$  flux densities from M32 are consistent with extrapolation of the photospheric emission from stars, taking  $B^T = 8.8$  mag and  $B - V \sim 0.9$  mag (ST). NGC 205 is a peculiar elliptical galaxy known to contain young blue stars (Hodge 1973). It is seen only at 60 and 100  $\mu\text{m}$ , corresponding to emission from 25 K dust.

V. CONCLUSIONS

1. M31 emits only a few percent of the stellar radiation at wavelengths greater than 10  $\mu\text{m}$ . The unobserved emission beyond 100  $\mu\text{m}$  may be as much as that observed between 10 and 100  $\mu\text{m}$ .
2. The IR emission is strongly concentrated in a ring with a semimajor axis of 45' and coincides in detail with the distribution of H II regions.
3. The radiation from the central part is due to hot dust heated by red giants in the bulge.
4. The companion elliptical galaxy M32 shows up at short wavelengths, consistent with emission from the photospheres

of evolved stars. NGC 205 shows up only at the longer wavelengths, and its emission is probably related to ongoing star formation.

*IRAS* would not have come alive in the Netherlands as an infrared satellite had it not been for the inspiration and the drive of Reinder van Duinen.

We acknowledge the development of special "destriping" and "flat-fielding" software by E. Kopan and K. Lugtenborg. We thank E. Brinks, R. Walterbos, P. Schwing, E. Berkhuijsen, and A. Bosma for various kinds of help and for discussions.

## REFERENCES

- Aaronson, M., Huchra, J., and Mould, J. 1979, *Ap. J.*, **229**, 1.  
 Baade, W. 1963, *Evolution of Stars and Galaxies*, ed. C. Payne-Gaposchkin (Cambridge: Harvard University Press), p. 56.  
 Beck, R., and Graeve, R. 1982, *Astr. Ap.*, **105**, 192.  
 Berkhuijsen, E. M., Wielebinski, R., and Beck, R. 1983, *Astr. Ap.*, **117**, 141.  
 Brinks, E., and Shane, W. W. 1983, *Astr. Ap. Suppl.*, in press.  
 Coleman, G. D., Wu, Chi-Chiao, and Weedman, D. W. 1980, *Ap. J. Suppl.*, **43**, 393.  
 Deharveng, J. M., Joubert, M., Monnet, G., and Donas, J. 1982, *Astr. Ap.*, **106**, 16.  
 de Jong, T., Clegg, P. E., Soifer, B. T., Rowan-Robinson, M., Habing, H. J., Houck, J. R., Aumann, H. H., and Raimond, E. 1984, *Ap. J. (Letters)*, **278**, L67.  
 Gallagher, J. S., and Hunter, D. A. 1981, *A. J.*, **86**, 1312.  
 Hildebrand, R. 1983, *Quart. J. R. A. S.*, **24**, 267.  
 Hodge, P. W. 1973, *Ap. J.*, **182**, 671.  
 ———. 1980, *A. J.*, **85**, 376.  
 Neugebauer, G., et al. 1984, *Ap. J. (Letters)*, **278**, L1.  
 Pellet, A., Astier, N., Viale, A., Courtes, G., Maucherat, A., Monnet, G., and Simien, F. 1978, *Astr. Ap. Suppl.*, **31**, 439.  
 Rieke, G. H., and Lebofsky, M. J. 1979, *Ann. Rev. Astr. Ap.*, **17**, 477.  
 Sandage, A., Becklin, E. E., and Neugebauer, G. 1969, *Ap. J.*, **157**, 55.  
 Sandage, A., and Tammann, G. A. 1981, *A Revised Shapley-Ames Catalog of Bright Galaxies* (Washington, D.C.: Carnegie Institution of Washington), Publication 635 (ST).  
 Telesco, C. M. and Harper, D. A. 1980, *Ap. J.*, **235**, 392.  
 Unwin, S. C. 1980a, *M. N. R. A. S.*, **190**, 551.  
 ———. 1980b, *M. N. R. A. S.*, **192**, 243.

## PLATE L6

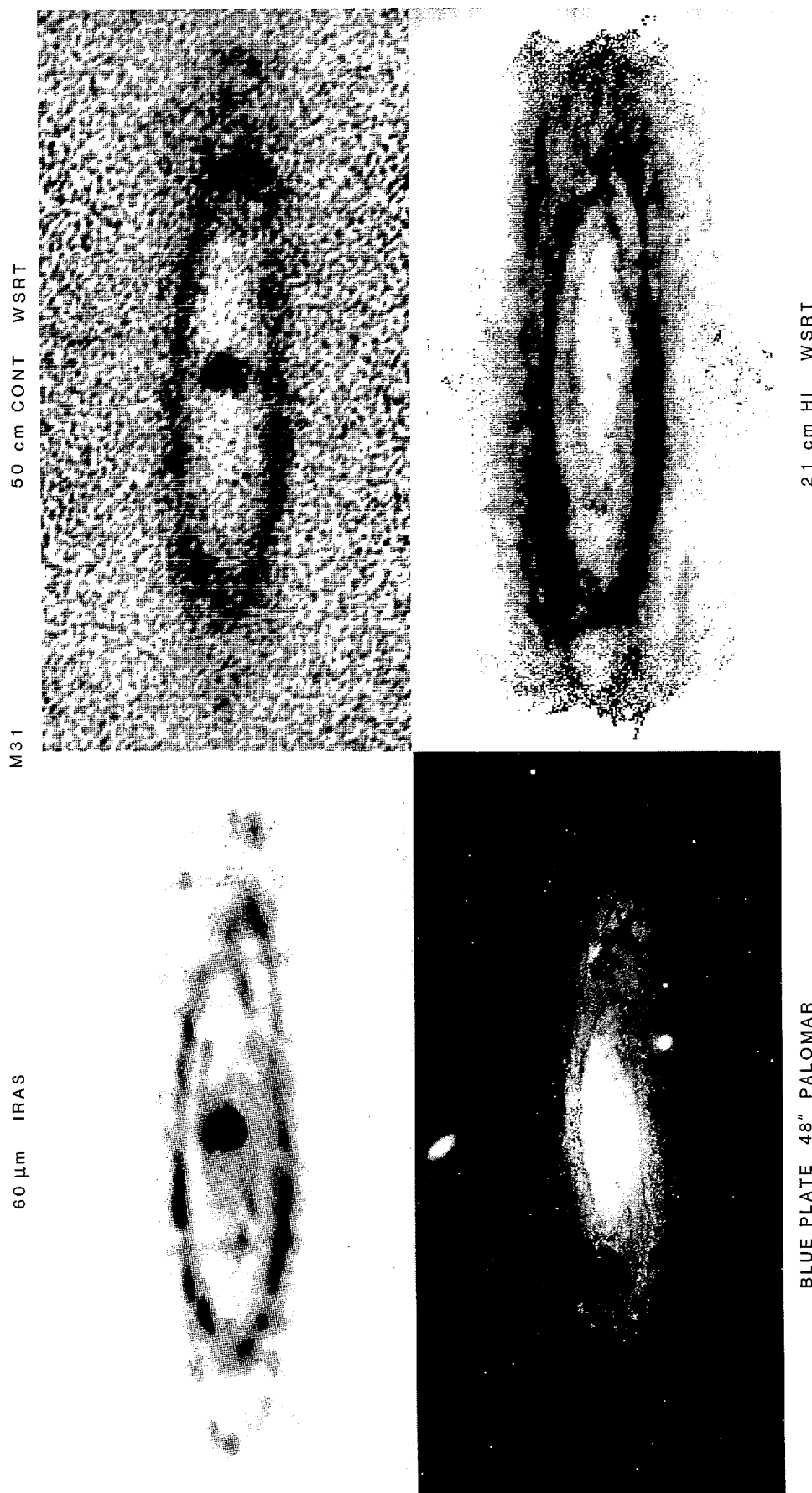


FIG. 2.—A montage of four maps of M31, each obtained at a different wavelength. (*upper left*) The 60  $\mu\text{m}$  IRAS map; (*upper right*) a map of the 50 cm continuum radiation; (*lower left*) a photograph in blue light; (*lower right*) a map in the 21 cm line of atomic hydrogen. The blue photograph has been taken with the 48 inch (1.2 m) Schmidt telescope (courtesy of Palomar Observatory). The two radio maps have been taken with the Westerbork Synthesis Radio Telescope (courtesy of Netherlands Foundation for Radio Astronomy).

HABING *et al.* (see page L59)